Neural, electrophysiological and anatomical correlates of temporal variability of brain networks and its implication in mental disorders

Temporal variability of brain networks: mechanism and characteristic alteration in mental disorders

SUMMARY

Functional connectivity in the brain has been shown to be dynamic in nature during resting state. Existing work usually investigate time-varying properties at micro (functional-connectivity) or macro (whole brain functional-connectivity) scale, and how meso-scale functional architecture of a brain region changes over time remains uncharted. Most importantly, the coupling between this variability of a region and its neuronal activity is hard to analyze at micro/macro scale, and the underlying mechanism remains elusive. We propose a variability measure that characterize the temporal change of the functional-connectivity profile of a region, which reflects the inclination of the ROI to dynamically reconfigure itself into multiple functional communities in different time. Whole-brain variability topography shows that that primary and unimodal sensory-motor cortices have lowest variability while transmodal areas demonstrate highest variability. Neural, electrophysiological and anatomical correlates analysis indicate that regional variability is modulated by both the amplitude/frequency of its BOLD activity and α band oscillation, and is relates to intra- versus inter-community structural connection. Application to schizophrenia, ADHD and Autism dataset including 1020 subjects revealed that regions demonstrate largest/smallest variability in controls are most liable to change in patients, and diametrically opposite patterns of variability changes are found among these 3 disorders. Our results indicate that healthy brain maintains an optimal level of the variability in key resting-state networks, which provide new insights into the dynamical organization of resting brain and how it alters in disordered brain.

ITRODUCTION

The human brain demonstrates remarkable variability in its structure and function (Frost and Goebel, 2012; Rademacher et al., 2001; Sugiura et al., 2007) , which underlies the inter-subject variability in thinking or behavior. For example, it has been shown that inter-subject variability in functional connectivity were heterogeneous across the cortex, and was significantly correlated with the degree of evolutionary cortical expansion (Mueller et al., 2013). Individual variability in resting-state functional

connectivity is also predictive of task performance (Baldassarre et al., 2012). Recently, the temporal variability of neuronal activity and functional brain connectivity/networks also attracts increasingly great attention (Calhoun et al., 2014; Kopell et al., 2014; Kucyi and Davis, 2014; Mueller et al., 2013; Tagliazucchi and Laufs, 2014). For example, BOLD signal variability which was considered measurement-related "noise", has significant age-predictive power (Garrett et al., 2010), and is related with task performance (Garrett et al., 2011). Using sliding window or time–frequency analysis, it is shown that even during rest, the spontaneous activity (Garrett et al., 2010, 2011; Lippe et al., 2009; McIntosh et al., 2008; Misic et al., 2010; Protzner et al., 2010; Samanez-Larkin et al., 2010) and the interactions among brain regions are dynamic, or nonstationary in nature (Chang and Glover, 2010; Hutchison et al., 2013; Kang et al., 2011; Majeed et al., 2011; Mueller et al., 2013).

To date most work on time-varying brain networks either focus on single functional connectivity among given ROIs (Chang and Glover, 2010; Hutchison et al., 2013; Kang et al., 2011; Kucyi and Davis, 2014; Majeed et al., 2011; Zalesky et al., 2014), or the connectivity of the whole brain (Allen et al., 2014). Variability at meso-scale, i.e., dynamic changes of the functional architecture of a given brain region has not been investigated. Though the presence nonstationarity in functional connectivity/networks has been revealed, the underlying mechanisms or the neural/anatomical correlates are still unknown. The advantage of characterizing simultaneous change of multiple functional connectivities associated with a brain region proposed in our paper is twofold: first, it allows the coupling between functional-connectivity variability of a region and local neural activity to be conveniently analyzed This helps delineate factors contributing to functional architecture changes of brain regions, shedding lights onto the mechanisms for variability. Second, it facilitates whole-brain topography of variability to be readily constructed so that the regions with significant variability changes in general mental disorders could be localized, helping us to understand the dynamics of functional brain networks for various mental disorders.

To this end, we propose to characterize the variability of functional architecture at brain region level using resting-state fMRI. This is achieved by constructing whole-brain functional networks at successive, non-overlapping time windows, and then compare the global functional-connectivity profile of a ROI across different windows. We hypothesized that variability of regional functional architecture may be modulated by local neural activity manifested in BOLD signal and α band oscillation in EEG, and has

its anatomical substrate. Using simultaneously recorded EEG and DTI data, we found that functiuonal-connectivity variability of a region is modulated by local BOLD activity (the amplitude and frequency of BOLD oscillations), and is positively associated with the alpha band power of the ROI. Moreover, variability is also related to the intra- versus. inter-community structural connectivity of a region. Application to different psychiatric disorders including schizophrenia, autism spectrum disorder, ADHD with their matched controls revealed disease-specific variability changes in DMN, visual and subcortical regions of the brain, which provides novel knowledge of spatial-temporal organization of brain and how it altered in patients with psychiatric disease.

Results

Variability of a region reflects the stability of its functional architecture/community membership change

Variability reflects collective changes of all the functional connectivities associated with a ROI with time. Low temporal variability (*V* near 0) means that the ROI's global functional connectivities are highly correlated at different time window, or alternatively, the correlation time series of the ROI with other regions are highly synchronized (Figure 1a and S1). On the contrary, the correlation time series of a high-variability ROI (*V* near 1) with other regions remains highly synchronous. In real fMRI data, due to the dynamical nature of functional connectivity, a ROI may connect with different regions, or be involved in different communities at different time slot. We find that the variability defined here can well characterize this property, see Fig. S2. Out of the 62 controls in dataset 1, 56 (90%) show negative correlation between regional variability and stability of intra-community members, 34 of which (55%) are significant ($p<0.05$). This means if the intra-community members of a ROI changes frequently with time (i.e., not stable, see Fig. S2 for detail), then the ROI will have a high variability. Therefore, regional variability reflects the ability/tendency of a region to reconfigure itself into different functional community with time, i.e., the membership changes.

Whole-brain variability topography and its robustness

For healthy controls, a non-uniform regional variability distribution throughout the cerebral cortex is found, see Figure 1 and Table S1. Various datasets consistently demonstrate low variability in primary sensory-motor (e.g., Heschl, postcentral and calcarine gyrus) or unimodal association

cortex (middle/superior occipital gyrus, cuneus, lingual gyrus, superior temporal gyrus), and default mode systems like medial frontal gyrus and PCC/PCUN. In comparison, transmodal association cortex, including limbic association cortex such as temporal pole, hippocampus , parahippocampus and amygdala (Bullard et al., 2013; Pearlson et al., 1996), anterior association cortex such as interior and orbital frontal gyrus, and posterior association cortex such as inferior parietal gyrus, inferior/middle temporal gyrus and paracentral lobule demonstrate high variability. The variability adopted demonstrates great robustness by showing consistent pattern in healthy controls across all 6 datasets (Figure S), though its amplitude differs slightly possibly due to age and other factors. Finally, note that the variability obtained at different window length (ranging from 20s to 40s) are highly correlated (Figure S4) and the above results are based on the average over different window length.

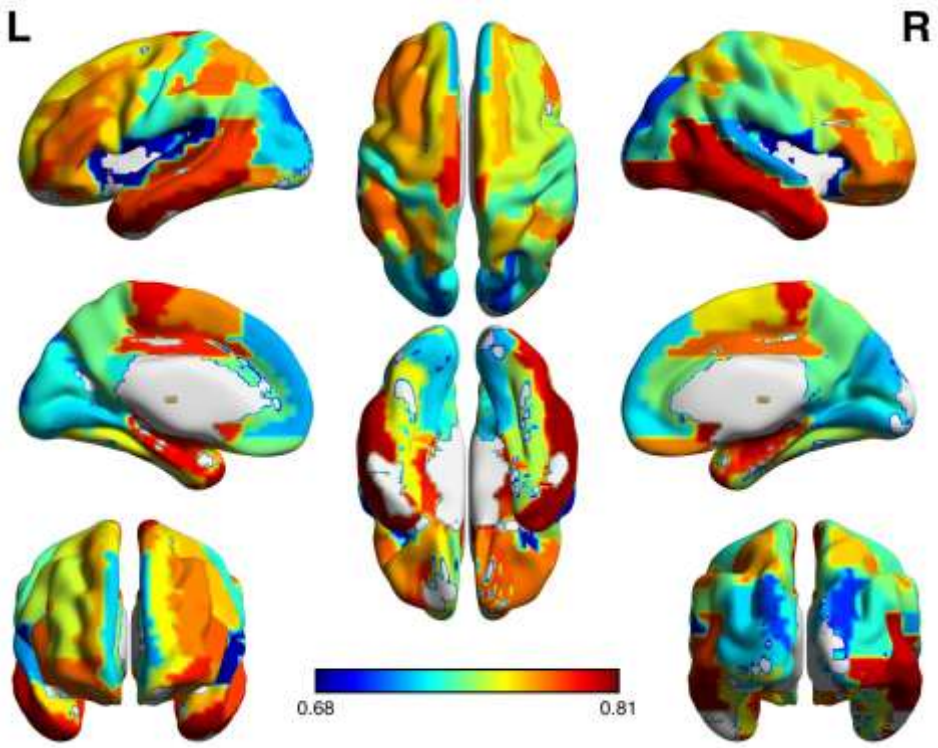

Figure 1 Whole brain variability topography on AAL template for healthy controls. The variability is averaged over the results obtained 6 different datasets.

Correlation between regional variability and local/global metrics from various modalities

BOLD activity

We first analyze correlation between regional variability and metrics derived from BOLD signal,

including BOLD activity (local, both its amplitude and low frequency components) and degree of the region (global, derived from BOLD brain network). We find that regional variability correlates negatively with both its BOLD activity and degree (naturally BOLD activity and degree are positively correlated), and it associates positively with low frequency energy, see Figure 2, S5, and Table S2 for details).

Electrophysiological recording

We used simultaneously recorded EEG/fMRI data and analyze the correlation between variability of a region with its alpha band power across subjects. We mainly found positive correlation between variability of a region and its α band power (8 out of 26 subjects, 31%), see Table S3.

Structural connectivity (DTI)

We define intra-community vs. inter-community structural connection ratio (IICR) characterizing if a node if more structurally to nodes within its own community. We find that out of 142 healthy subject in IMAGEN dataset, IICR is significantly correlated with variability across 90 regions for 49 subjects ($p<0.05$). 40 of them (28%) show a negative correlation (-0.28 ± 0.0032). This suggests that the more intra-community connections a node has (compared to intra-community connections), the smaller its variability. This is reasonable as the node with more fiber connection to regions belonging to the same community is expected to form more stable functional community and that its variability is low. In comparison, a node that is structurally connected to regions from many other communities is expected to have a large variability because the membership changes would be more frequent.

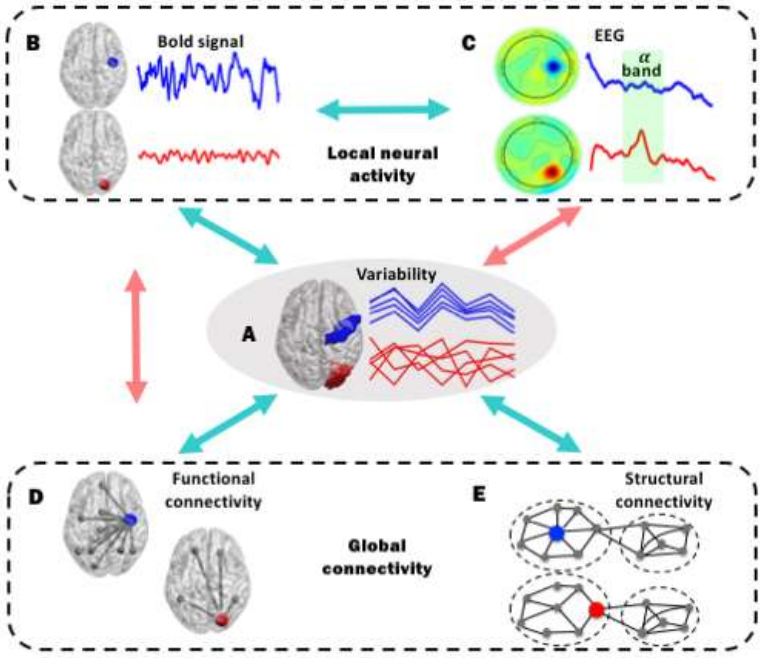

Figure 2 Correlation between regional variability and local/global metrics obtained from various modalities (blue for negative correlation and red for positive correlation, with the strength of correlation listed in Table S2). **A.** Variability of a ROI. The top panel denotes a ROI with small variability, and the correlation coefficient time series of the ROI with the rest region are synchronous. The bottom panel is for a ROI with large variability, and its correlation time series with other regions are independent. **B.** Amplitude of BOLD activity of a ROI. Top panel for large amplitude and the bottom for small amplitude. **C.** α band power of EEG of a ROI. Top panel shows a region with small α band power and the bottom panel for a region with large α band power. D. Degree of a ROI obtained from BOLD-constructed brain network. Top panel shows a region with large degree and the bottom panel for a region with small degree. **E**. intra-community vs. inter-community structural connection ratio (IICR). Top panel shows a region with large IICR (i.e., the ROI connect more with nodes belonging to the same community, and the bottom panel for a region with small IICR (the ROI connect more with nodes belonging to different community. The upper (lower) panels in each figure are correlated, i.e., a region with low variability will have a higher BOLD activity, high degree, low α band oscillation and high IICR.

Characteristic changes of variability in various mental disorders

We furthermore performed a whole brain variability analysis across healthy controls and subjects with schizophrenia, Autism spectrum disorders (ASD) and ADHD and identified disease-specific changes. For the disorders with more than one datasets, meta-analysis is adopted to integrate results from multi-dataset. For schizophrenia, more than 20% of brain regions (19) show significant variability difference, see Figure 3a and Table S4a. The variability decreases mainly in rectus, para-hippocampus and temporal lobe (middle temporal pole and inferior temporal gurus), while increases most prominently in subcortical areas like thalamus and parllidum, putamen, and visual cortex involving superior occipital and lingual gyrus. Thalamic variability are found to be associated with positive symptoms, see Table S5a.

For autisms, all regions showing significant variability changes are found to have a higher variability in autism patients (compared to controls), most significantly in medial orbital and superior medial frontal gyrus , see Figure 3b and Table S4b. In particular, the variability of these default network regions are found to be positively related to the symptom scores (Table S5b).

For ADHD, we found that medial orbital frontal gyrus, PCC/PCUN, angular (DMN network) have higher variability in ADHD patients, while the brain regions in subcortical network, i.e., bilateral caudate and thalamus are lower in ADHD patients than controls, see Figure 3c and Table S4c. Variability changes in post cingulate and frontal regions are found to be associated with severity of ADHD symptoms, see Table S5c.

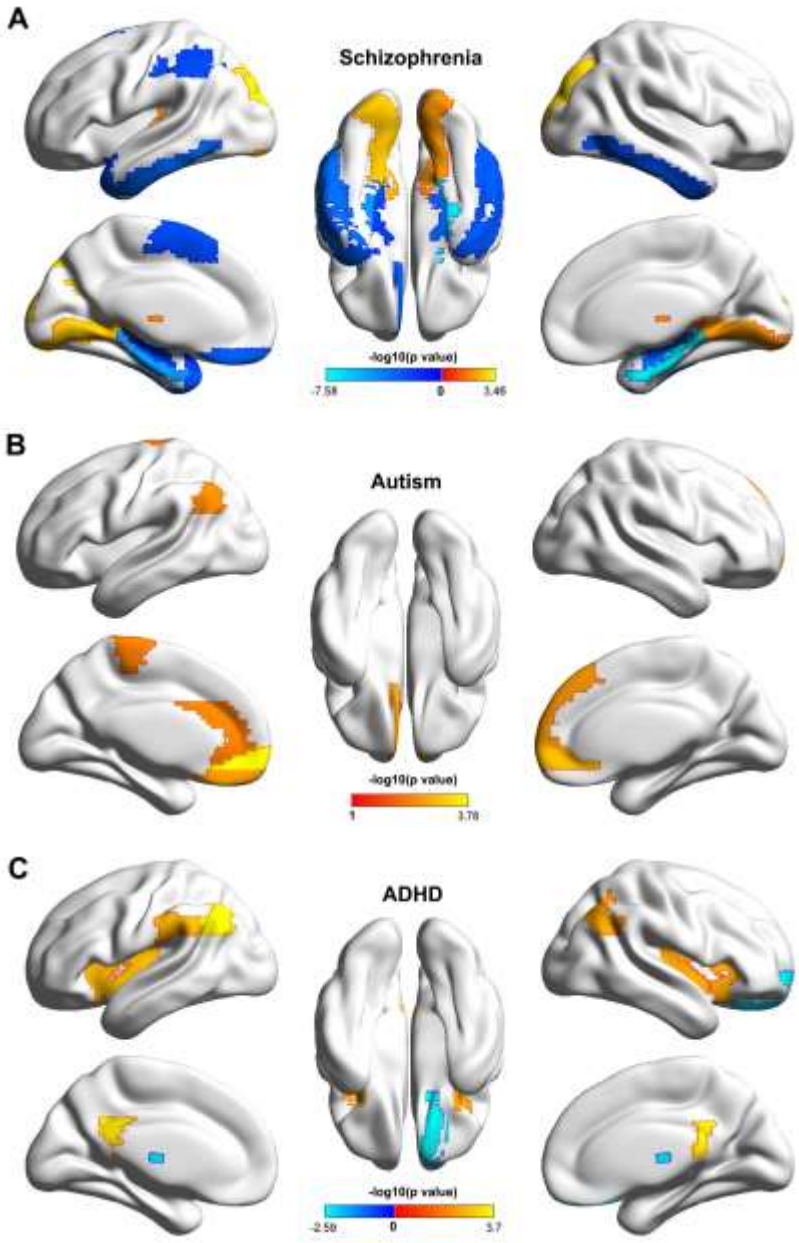

Figure 3 Brain regions showing significant variability difference across patients with mental disorders and matched controls. A. Schizophrenia; B. Autism; C. ADHD. Blue indicates variability of patients is lower than that of controls, and red indicates the opposite.

Discussion

Neural, electro-physiological and anatomical correlates of variability

Interestingly, the primary (Heschl and postcentral gyrus, superior occipital gyrus) or unimodal association cortex (middle occipital gyrus, cuneus, calcerine and lingual gyrus, superior temporal gyrus) were found to show very low variability (see Figure 1). This is because these regions are involved in

unitary neural circuit responsible for simple sensory-motor functions, and the regions they connect remains are rather stable over time. In comparison, the transmodal areas (Mesulam, 1998) including all heteromodal (anterior association cortex like interior frontal gyrus, triangular part posterior association cortex such as inferior parietal gyrus, paracentral lobule), paralimbic (temporal pole, parahippocampus) and limbic areas (hippocampus and amygdala) demonstrate high variability. This is because trans/heteromodal cortex receives information from multiple sensory modalities and are considered to be responsible for more complex or integrated cognitive activities (Bullard et al., 2013; Pearlson et al., 1996). Therefore these regions may take part in multiple functional communities in different time and have high variability. We also note relatively low-variability of DMN network, including medial frontal gurus and post cingulate/precuneus due to the strong connection within this network. These results are consistent with (Power et al., 2011) that suggests sensory-motor, visual and default mode systems are rather stationary.

Certain brain region such as caudate is known to be involved in multiple neural circuits, also has a large variability that facilitate more flexible engagement of a region into various circuit, reflecting its ability to dynamical reconfigure itself into multiple functional circuits.

The negative correlation between intra- vs. inter-community structural connection and variability (Figure 1e) support the above conclusion. If structural connection of a region is confined only to its own community, then it will be stably involve one functional community and its variability would be low. In comparison, a region with structural connection to multiple communities are bound to switch among different functional circuit thus demonstrates a high variability.

The negative correlation between variability of a region and its BOLD activity /degree (Figure 2 and Table S2) indicates that the variability is modulated by the local BOLD activity (both strength of BOLD oscillation and its frequency). To facilitate information transmission, or functional integration with other regions, it is natural for a brain region to demonstrate greater BOLD activity and relatively high level of functional connectivity/functional integration with other regions, therefore higher degree. In this case, the variability of the ROI is expected to be low to maintain a high level of information transmission.

The negative correlation between a ROI's variability and low frequency component in its BOLD oscillation indicates that low frequency oscillation of a region facilitate information transmission and functional integration: a low-variability ROI has higher low-frequency component, therefore tends to

synchronize easily with other regions. This is consistent with the finding that lower frequency oscillations allow for integration of large neuronal networks (Buzsaki and Draguhn, 2004). Comparatively, a region with more high-frequency components usually cannot synchronize effectively with other regions, thus demonstrate high variability.

The variability of a region is also modulated by α band power of its EEG, manifested by the positive correlation between variability and α power (Figure 2 and Table S2). This is consistent with the finding that αoscillation inhibits BOLD activity by showing a strong negative correlation with BOLD activity, especially in occipital, parietal and frontal cortical (de Munck et al., 2007; Laufs et al., 2006) Considering the negative correlation between BOLD activity regional variability, a positive correlation between variability and α power is expected, which is verified in our work.

Characteristic changes in temporal variability in various mental disorders

Resting-state functional connectivity have revealed alterations in the intrinsic topographical organization of brain in several mental disorders, including schizophrenia, autism and ADHD (Castellanos et al.; 2008;Kennedy and Courchesne, 2008; Whitfield-Gabrieli and Ford, 2012). However, little attention is devoted to time-varying networks in disease (Damaraju et al., 2014; Ma et al., 2014). Our work demonstrate disorder-specific changes in variability, which might add important further information on the specific, dynamical neuropathological profiles of the different mental disorders, and contribute to the development of differential & diagnostic imaging.

Previous studies in schizophrenia reported a hyper-activated and concomitantly hyper-connected DMN (Whitfield-Gabrieli et al., 2009) , which may mirror intensive self-reference and decreased attentional capacities in patients (Whitfield-Gabrieli et al., 2009). In line with these findings, schizophrenia patients exhibited decreased variability in the DMN, which was associated with increased activity and connectivity. The interplay between the DMN and the task-positive network is related to working memory and switching between an intrinsic and extrinsic focus of attention (Weissman et al., 2006; Whitfield-Gabrieli and Ford, 2012). Decreased default mode system variability in schizophrenia patients therefore relate to schizophrenia-characteristic neurocognitive symptoms, e.g., an exaggerated focus on one's own thoughts and feelings, and a blurring of the boundary between internal and external world (Whitfield-Gabrieli et al., 2009). Schizophrenia also demonstrate basic information processing deficits, particularly sensory gating (Bender et al., 2007) associated with thalamus. Increased variability in schizophrenia patients in subcortical regions could therefore point to de-synchronized basic filter

modules, associated with an inability to filter out irrelevant stimuli and a correspondingly diminished ability to focus attention (Freedman et al., 1987).

Our results are consistent with Yu (Yu et al., 2014), who showed greater oscillation in the slow-5 band (0.01-0.027 Hz, corresponding to low frequency in our paper) than in the slow-4 band (0.027-0.073 Hz, corresponding to high frequency) in mPFC while greater ALFF/fALFF in the slow-4 band in subcortical regions like basal ganglia. We find that schizophrenia patients demonstrate lower variability in frontal regions corresponding to higher low frequency oscillations), and higher variability in thalamus/basal ganglia corresponding to smaller low-frequency component (0.027-0.073).

For autisms, a number of works have found reduced DMN connectivity and activity (Kennedy and Courchesne, 2008) in resting-state, which correspond to high variability of DMN regions in our work. High variability of DMN network suggests a low functionality, i.e., disruption of the resting-state default-mode cognition, which is mainly related to self-referential processing, such as processing of information associated with theory of mind, inner speech, retrieving and manipulating memories, and future plans (Garrity et al., 2007; Greicius et al., 2003; Kennedy et al., 2006). Therefore there might be an absence of self-referential thought in autism (Cherkassky et al., 2006), which is directed more towards obsessive interests and sensory-enviroment processing than towards self-reflective activities for autism patient (Crespi and Badcock, 2008).

Temporal variability analysis in ADHD patients revealed increased variability in the DMN and concomitantly decreased variability in subcortical regions. In accordance with our findings previous studies have reported decreased DMN connectivity and integration (Castellanos et al., 2008) in ADHD, subsumed under the "default-mode interference" hypothesis (Castellanos et al., 2008; Sonuga-Barke and Castellanos, 2007). This theory suggests that the characteristic pattern of variability in performance in ADHD may be based on a dysfunctional synchronization in the DMN or its interactions with "task-active" regions, e.g., decreased anti-corelations between the PCC and task-positive regions (the dACC, Castellanos et al., 2008). This is consistent with our finding of high variability in DMN regions like PCC/PCUN (associated with its low functional connectivity), which may reflect default mode interference that contributs to attentional deficits in ADHD. In particular, the high variability with PCC/PCUN may be related to diminished volume (Carmona et al., 2005) or decreased cortical thickness (Makris et al., 2007) in precuneus and PCC in ADHD.

Two interesting trend is worthy to note. First, regions demonstrating vary high/low variabilities in healthy

controls are most liable to change in psychiatric disorders. As is shown in Table S4. About half of the significantly changed regions in the 3 disorders are among the top 10% highest- or lowest-variability regions in matched controls (11/19 in schizophrenia, 3/8 in autism, and 4/10 in ADHD). This indicates that regions at the two extremes of the axis of variability are not stable and tend to be affected by mental disorders. Second, the three different mental disorders showed disease-specific, partly opposite regional pattern of altered variability in regions previously reported to associate with the symptoms. For example, schizophrenia and Autism demonstrates opposite trend in variability changes in DMN regions (compared with respective controls, see Figure 1 and Table S6). This is consistent with the idea that schizophrenia and autism may represent opposite pathologies (Crespi and Badcock, 2008). These disorders exhibit diametrically opposite phenotypes, or patterns for characteristics of social brain development, like social cognition, language, and behavior, and local /global processing. Social cognition is believed to be underdeveloped in autistic-spectrum disorders, while hyper-developed on the psychotic spectrum (Crespi and Badcock, 2008). In addition, there is also opposite trend in variability changes in thalamus for schizophrenia and ADHD (Figure 1 and Table S6).

The influence of head motion

Though it has been shown that head movements can influence estimates of functional connectivity (Power et al., 2014), there are also evidence that head movement only explains a small fraction of the variability in connectivity (Van Dijk et al., 2012), and motion-associated differences in brain connectivity cannot fully be attributed to motion artifacts but rather also reflect individual variability in functional organization (Zeng et al., 2014). To evaluate the possible effect of head motion on the regional variability, we calculate their correlation, see Table S7. Out of the 6 fMRI datasets, only the patients in dataset 4[#] (ADHD: NYU) show significant correlation with head movements (FDR, q=0.05). We also listed the regions whose *p* value is less than 0.01 for other datasets in Table S7, which we find to have no consistent patterns across datasets. These results suggests that the head movement effect may be small, and in the case-control study of ADHD we did not use NYU dataset due to the correlation with headmovement.

EXPERIMENTAL PROCEDURES

Quality control

For each psychiatric disorders, we combine multi-center data with possibly large variation. Therefor we set up a protocol to ensure data quality. The exclusion criteria were: 1. Subjects with poor

structural scans, or functional MRI data cannot be successfully preprocessed, i.e., normalization to MNI space, or without complete demographic information. 2. Head movement: subjects with >10% displaced frames in a scrubbing procedure or maximal motion between volumes in each direction >3 mm, and rotation about each axis > 3° were excluded. Patients and controls were screened in each dataset so that the total root mean square displacements did not show significant differences. It should be noted that for ADHD dataset, we only have the preprocessed data (i.e., BOLD time series) from the public website, thus scrubbing cannot be performed. 3. For autism dataset, subjects with a full IQ exceeding 2 standard deviations (SD) from the overall ABIDE sample mean (108 _ 15) were not included.

1. Case-control study (fMRI)

Subjects

Six resting-state datasets were used from Schizophrenia, Autism and ADHD patients and their respective healthy control groups. Full demographic details of patients and healthy controls is given by Table 1, and medication information are given in Table S8.

Schizophrenia

Two datasets were used, including Taiwan dataset (1# dataset: 62 healthy controls and 69 medicated schizophrenia patients) from National Taiwan University Hospital in Taiwan (Guo et al., 2014) and COBRE dataset from the Center for Biomedical Research Excellence (COBRE, 2# dataset: 67 healthy controls and 53 chronic patients).

All patients were identified according to DSM-IV diagnostic criteria by qualified psychiatrists and symptom severity assessed using the Positive and Negative Syndrome Scale (PANSS). Exclusion criteria included (1) presence of other DSM-IV disorders; (2) history of substance abuse; (3) clinically significant head trauma. Healthy controls were also confirmed using DSM-IV criteria to be free of schizophrenia or other Axis 1 disorders and not to have a history of substance abuse or clinically significant head trauma. Informed consents were approved by Institutional review boards (IRB) of respective hospitals (Taiwan and USA).

Autism

The autism datasets is from The ABIDE repository hosted by the 1000 Functional Connectome Project (http://fcon_1000.p rojects.nitrc.org for more information). In this paper we used datasets from two centres, i.e., NYU (3# dataset: 102 controls and 75 patients) and UM (4# dataset: 64 controls and 38

patients). Research procedures and ethical guidelines were followed in accordance with the Institutional Review Boards (IRB) of the respective participating institution. Details of diagnostic criteria, acquisition, informed consent, and site-specific protocols are available at : http://fcon_1000.projects.nitrc.org/indi/abide/.

ADHD

The ADHD dataset was obtained from the ADHD-200 Consortium (http://fcon_1000.projects.nitrc.org/indi/adhd200/). 2 sites with a total of 490 subjects were used, involving PKU dataset (5# dataset: 143 controls and 99 ADHD patients), and NYU dataset (6# dataset:108 controls and 140 ADHD patients). All subjects were evaluated using the Schedule of Affective disorders and Schizophrenia for Children - Present and Lifetime version (KSADS-PL) with one parent for the establishment of diagnosis. The ADHD Rating Scale (ADHD-RS) IV was employed to measure severity of ADHD symptoms. All subjects are (1) right handed, (2) no history of head trauma with loss of consciousness (3) no history of neurological disease or diagnosis of schizophrenia, affective disorder, pervasive development disorder or substance abuse (4) had a Weschler Intelligence Scale for Children score of >80. Details of diagnostic criteria, acquisition, informed consent, and site-specific protocols are available at : http://fcon_1000.projects.nitrc.org/indi/adhd200/.

2. Simultaneous EEG/fMRI recording

26 healthy subjects (7 # dataset :11 females, age 21.4 ± 2.0, between 18 and 25 years) without any history of psychiatric or neurological illness were recruited from the local community (approved by the Ethics Committee of the Southwest University) for acquisition of simultaneous resting-state EEG/fMRI, which is used in electrophysiological correlate analysis of variability. Written informed consent was obtained after detailed explanation of the study protocol.

3. fMRI/DTI

142 healthy subject (7 # dataset: 76 females, age 14.5±0.2, between 13.2 and 15.9 years) with both resting-state and DTI images from IMAGEN consortium (Schumann et al., 2010) were used to seek anatomical correlates of variability. The detailed information can be found in (Schumann et al., 2010).

Image acquisitions

1. Case-control study

All Individuals were asked to remain still, close their eyes (For COBRE and UM (autism) dataset, eye open/close information were not available) and think of nothing systematically but not to fall asleep when functional imaging data were collected.

Schizophrenia

For Taiwan dataset, a 3T MR system (TIM Trio, Siemens) is used. A total of 180 volumes of EPI images were obtained axially, (slices, 34; TR, 2000 ms; TR, 24 ms; thickness, 3 mm; flip angle, 90°; FOV, 256×256 mm2; resolution, 64 ×64).

For COBRE dataset, BOLD fMRI were obtained by single-shot full k-space EPI with ramp sampling correction using the inter-comissural line (AC-PC) as a reference (TR: 2 s, TE: 29 ms, matrix size: 64x64, 32 slices, voxel size: 3 × 3 × 4 mm3 FOV = 256x256 mm2).

Autism

All data In the ABIDE initiative being collected at a number of different centres with 3T scanners. Details regarding data acquisition are provided on the ABIDE website (http://fcon_1000.projects.nitrc.org/indi/abide).

ADHD

Peking University: SIEMENS TRIO 3-Tesla. A total of 232 volumes of echo planar images were obtained axially (30 slices; TR 2000 ms; TE 30 ms; slice thickness 4.5 mm; flip angle 90°; FOV 220×220 mm2; matrix 64×64).

New York University: A total of 172 volumes of echo planar images were obtained axially (33 slices; TR 2000 ms; TE 15 ms; slice thickness 4 mm; flip angle, 90°; FOV = 240×240 mm^2; matrix 80×80).

2. Simultaneous EEG/fMRI recording

The EEG was digitized at 5 kHz, referenced online to FCz using a non-magnetic MRI-compatible EEG system (BrainAmp MR plus, Brain products, Munich, Germany). 32 electrodes (nonmagnetic Ag/AgCl) were placed on the scalp according to the international 10/20 system. An additional electrode was dedicated to the electrocardiogram. BOLD fMRI was acquired using a 3T Siemens Trio scanner. 200 functional volumes were scaned using an EPI sequence with the following parameters: TR/TE=1500/29

ms, FOV=192×192 mm^2, flip angle=90°, acquisition matrix=64×64, thickness/gap=5/0.5 mm, in-plane resolution=3.0×3.0 mm^2, axial slices=25.

3. fMRI/DTI

As the resting-state fMRI and DTI data are from multi centers, the detailed parameters can be found in Imagen consortium (Schumann et al., 2010).

Data preprocessing

fMRI data

For all fMRI data used in our study, the first 10 volumes were discarded to allow for scanner stabilization and the subjects' adaptation to the environment. fMRI data preprocessing was then conducted by SPM8 (http://www.fil.ion.ucl.ac.uk/spm) and a Data Processing Assistant for Resting-State fMRI (DPARSF). The remaining functional scans were first corrected for within-scan acquisition time differences between slices and then realigned to the middle volume to correct for inter-scan head motions. Subsequently, the functional scans were spatially normalized to a standard template (Montreal Neurological Institute) and resampled to 3× 3 ×3 mm^3. After normalization, BOLD signal of each voxel was firstly detrended to abandon linear trend and then passed through a band-pass filter (0.01-0.08 Hz) to reduce low-frequency drift and high-frequency physiological noise. Finally, nuisance covariates including head motion parameters, global mean signals, white matter signals and cerebrospinal signals were regressed out from the BOLD signals. After data preprocessing, the time series were extracted in each ROI by averaging the signals of all voxels within that region. In terms of Global signal removal, please see supplemental experimental procedure for and Fig. S6 for comparison between Global signal removal and unremoval.

We further implemented careful volume censoring (‘scrubbing’) movement correction (Power et al., 2014) to ensure that head-motion artefacts were not driving observed effects. The mean framewise displacement was computed with the framewise displacement threshold for exclusion being a displacement of 0.5 mm. In addition to the frame corresponding to the displaced time point, one preceding and two succeeding time points were also deleted to reduce the ‘spill-over’ effect of head movements. Finally, we used the mean framewise displacement as a covariate when comparing the two groups during statistical analysis.For all three datasets the automated anatomical labeling atlas (AAL) (Tzourio-Mazoyer et al., 2002) was used to parcellate the brain into 90 regions of interest (ROIs) (45 per

hemisphere). The names of the ROIs and their corresponding abbreviations are listed in Table S9.

Simultaneous EEG/fMRI data processing

EEG data was preprocessed by temporal independent component analysis to remove gradient and ballistocardiographic (BGC) artifacts (Mantini et al., 2007). The FMRIB toolbox in EEGLAB (www.sccn.ucsd.edu/eeglab) was used for correction of the MRI imaging artifact (Niazy et al., 2005). It implements the adaptive artifact subtraction (AAS) method, in which the MRI imaging artifact waveforms are segmented, averaged and iteratively subtracted from the EEG signals (Allen et al., 2000). Subsequently, data were down-sampled to 250 Hz, filtered within the 1-30 Hz frequency band (Chebyshev II-type filter, 40 dB attenuation, zero-phase distortion). Data segments contaminated by muscle activity were removed, and 190 to 275 s (225 ± 32 s) of continuous EEG recordings were remained. A digital FFT-based power spectrum analysis (Welch technique, Hanning window, no phase shift) computed power density of the EEG rhythms. The following standard band frequencies were studied based on previous EEG studies (Lukas et al., 1986; Sanz-Martin et al., 2011): delta (2–4 Hz), theta (4–8 Hz), alpha 1 (8–10.5 Hz), alpha 2 (10.5–13 Hz), beta 1 (13–20 Hz), and beta 2 (20–30 Hz).

DTI Processing

We first used FMRIB Software Library v5.0 (http://fsl.fmrib.ox.ac.uk/fsl) [Jenkinson et al., 2012] to remove the eddy-current and extract the brain mask from the B0 image. Then, we used TrackVis [Wang et al. 2007] to obtain the fiber images by the deterministic tracking method, and the anatomical regions were defined using the automated anatomical labelling atlas (AAL) (Tzourio-Mazoyer et al., 2002)，based coregistered T1 image from each subject. This way the presence of streamlines connecting every pair of brain regions. All the processes were performed using the PANDA suite (Cui et al., 2013). Finally, for any pair of brain regions, we will have fractional anisotropy, fiber number and fiber length assigned to the corresponding fiber connections.

Table **1:** Demographic information for the 6 dataset involving 3 psychiatric disorders (a) schizophrenia, (b) Autism and (c) ADHD.

(a) Schizophrenia

1. Taiwan dataset

Groups	N	Age/yrs	Sex (M/F)	PANSS (P)	PANSS (N)	PANSS (G)	Illness duration
Taiwan							
Controls	62	29.9±8.6	25/37				
Schizophrenia	69	31.9±9.6	35/34	11.9±4.7	13.6 ±6.3	27.±9.6	7.2±6.6
COBRE							
Controls	67	34.8 ± 11.3	42 / 11				
Schizophrenia	53	36.8 ± 13.7	46 / 21	14.9±4.6	14.7±5.2	29.7±8.2	8.9±6.9

(b): Autism

Groups	N	Sex (M/F)	Age/yrs	Hamilton score
NYU				
Controls	102	76/26	15.9± 6.3	21.4±12.7
Autism	75	65/10	14.8±7.0	92.6±31.0
UM				
Controls	64	48/16	15.1±3.7	
Autism	38	31/7	13.6±2.4	

(c) ADHD

Dataset	N	Age/yrs	Sex (M/F)	ADHD index
PKU				
Control	143	11.4±1.9	84/59	29.3±6.4
ADHD	99	12.1±2.0	89/10	50.4±8.2
NYU				
Control	108	12.2±3.1	54/54	45.4±6.0
ADHD	140	11.1±2.7	106/34	71.9±8.7

Methods

Temporal variability of a brain region

To characterize temporal variability of functional connectivity profile of a given region, we first segment all BOLD time series into *n* non-overlapping windows each with length *l*. Within the *i*th time window the whole-brain functional network F_i (which is a *m*m* matrix, with *m* nodes) is obtained, The correlation map (or functional connectivity profile) for a brain region *k* at time window *i* then is F_i (*k*,:) which is a *m*-dimensional vector and is shortened as $F_{i,k}$. We then define the variability of a ROI *k* as:

$V_k = 1 - E\left[corrcoef\left(F_{i,k}, F_{j,k}\right)\right], i, j = 1,2,3, \dots, n$, see Figure 3 for illustration.

The latter part compares the global functional connectivity profile of a region across different time windows, which is the averaged correlation coefficient among different functional-connectivity profiles of a region and thus a similarity measure. A deduction from 1 then indicates temporal variability of a region. By this we are able to evaluate temporal variability of a ROI at the network level, and localize to a specific brain region simultaneously. In fact this measure was used at a different context in (Baldassarre et al., 2012) to calculate individual variability, i.e., the correlation is performed among global functional connectivity profile for different individual, rather than among global functional connectivity profiles obtained at different time window for the same individual. To reduce the effect of segmentation scheme of BOLD signal, for a given window length *l*, we perform *l*-1 times segmentation and each time we start from the *s*th point (s=1,2,…, *l*-1) and average the variability obtained from *l*-1 times segmentation. in application to avoid arbitrary choice of window length, we calculate V_k at different *l* (l=10, 11, 12,…20 sampled points, equal to 20, 22, 24,…40 second), and then take the average value as the final variability of the ROI. We choose the above window length as it was suggested that window sizes around 30–60 s produce robust results in image acquisitions, cognitive states (Shirer et al., 2012) and topological descriptions of brain networks (Jones et al., 2012). In fact we find that variability obtained at different window length (e.g., 20s, 30s, 40s) are highly correlated (r>0.98, Figure S4), indicating that this metric does not critically depend on the choice of window length.

Correlation between variability and local/global characteristics from multi-modalities

To elucidate the neural/electrophysiological and anatomical correlates of temporal variability, we perform extensive correlation analysis using simultaneously collected EEG/fMRI (dataset 5$^{\#}$) and fMRI/DTI (dataset 7$^{\#}$) data of healthy controls. For neural correlates, correlation between variability of a region and its BOLD activity (local measures, including the standard deviation of BOLD signal and its low frequency component) and degree (global measure, the number of its functional connectivity with

absolute strength larger than 0.3) across 90 brain regions for each subject. For electrophysiological correlates, we perform correlation between variability of a region and its α band power (obtained from simultaneously recorded EEG) across all 28 electrodes/regions (see Supplemental Experimental Procedures for the correspondence to the 28 regions in AAL template) for each subject.

For anatomical correlates, we perform correlation between variability of a region and its intra-community vs. inter-community structural connection ratio (IICR) across 90 brain regions for each subject. IICR is defined as the total number of fibers of the ROI with those regions belonging to the same community divided by the total number of fibers with those regions belonging to other communities. It characterizes the specificity/selectivity of a ROI to structurally connect to regions belong to its own functional community (see Supplemental Experimental Procedures).

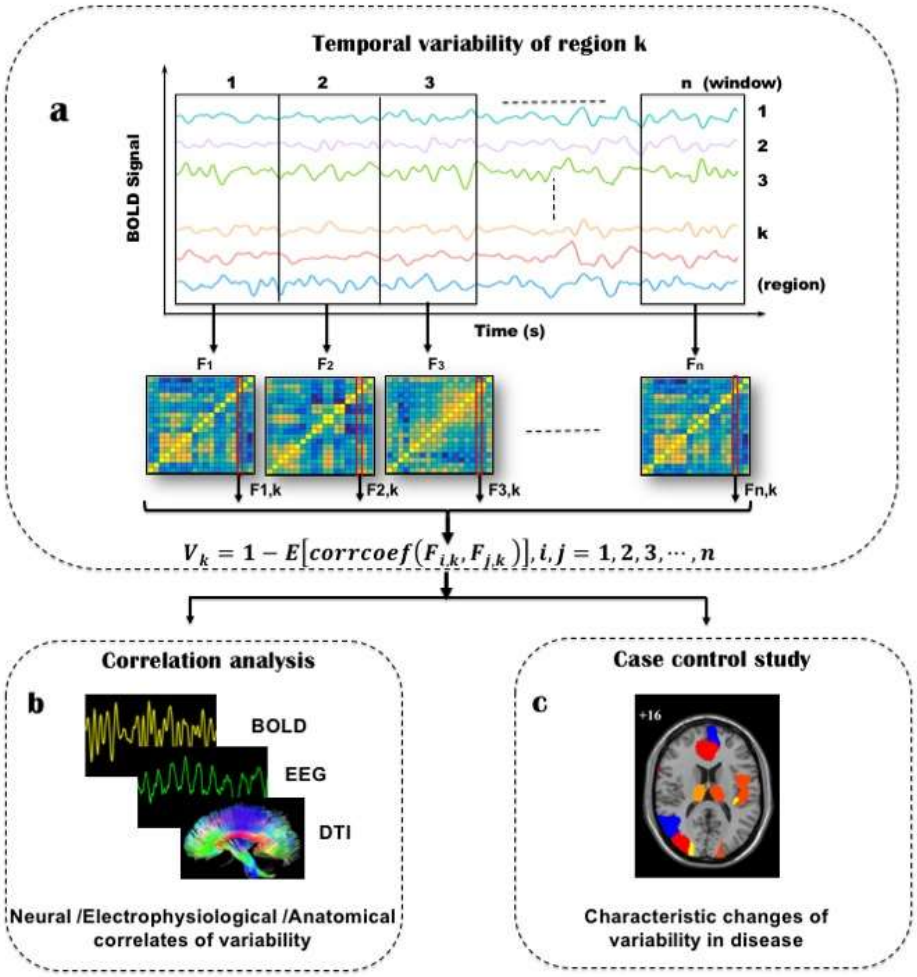

Figure 3. Flow chart of temporal variability analysis (a) The procedure of calculating variability of a given region. (b) Correlation analysis of variability with measures from multimodalities neuroimaging

data like simultaneously recorded EEG and DTI data. (c) Case-control studies for different psychiatric disorders including schizophrenia, autism and ADHD.

Meta-analysis to integrate results from different imaging centers

In case-control studies, we used a Liptak-Stouffer z-score method (Liptak, 1958) which is well-validated in integrating results from individual datasets (e.g., MRI (Glahn et al., 2008)). For datasets of the same mental disorder, the p-value of each functional connectivity in the relevant dataset *i* was converted to the corresponding z score: $z_i = \Phi^{-1}(1 - p_i)$, where Φ is the standard normal cumulative distribution function. Then a combined *z* score for a functional connectivity was obtained using the Liptak-Stouffer formula:

$$Z = \frac{\sum_{i=1}^{k} w_i z_i}{\sqrt{\sum_{i=1}^{k} w_i^2}}$$

where w_i is the inverse of the variance of z_i. Z follows a standard normal distribution under the null hypothesis and is transformed into its corresponding p-value, with Bonferroni correction used to correct for multiple comparisons.

Author Contributions

"A.B. and C.D. conducted the experiments, E.F. designed the experiments JZ wrote the paper…"

SUPPLEMENTAL INFORMATION

Supplemental Information includes Supplemental Experimental Procedures, 6 figures, and 9 tables.

Acknowledgement

J.Zhang is supported by National Science Foundation of China (NSFC 61104143 and 61573107), and special Funds for Major State Basic Research Projects of China (2015CB856003). J.Feng is a Royal Society Wolfson Research Merit Award holder, partially supported by the National High Technology Research and Development Program of China（No. 2015AA020507) and the key project of Shanghai Science & Technology Innovation Plan (No. 15JC1400101), the National Centre for Mathematics and Interdisciplinary Sciences (NCMIS)

of the Chinese Academy of Sciences and Key Program of National Natural Science Foundation of China (No. 91230201).

Reference

Allen, E.A., Damaraju, E., Plis, S.M., Erhardt, E.B., Eichele, T., and Calhoun, V.D. (2014). Tracking Whole-Brain Connectivity Dynamics in the Resting State. Cereb Cortex 24, 663-676.

Allen, P.J., Josephs, O., and Turner, R. (2000). A method for removing imaging artifact from continuous EEG recorded during functional MRI. Neuroimage 12, 230-239.

Bak, N., Rostrup, E., Larsson, H.B., Glenthoj, B.Y., and Oranje, B. (2013). Concurrent functional magnetic resonance imaging and electroencephalography assessment of sensory gating in schizophrenia. Human brain mapping.

Baldassarre, A., Lewis, C.M., Committeri, G., Snyder, A.Z., Romani, G.L., and Corbetta, M. (2012). Individual variability in functional connectivity predicts performance of a perceptual task. P Natl Acad Sci USA 109, 3516-3521.

Becker, B., Mihov, Y., Scheele, D., Kendrick, K.M., Feinstein, J.S., Matusch, A., Aydin, M., Reich, H., Urbach, H., Oros-Peusquens, A.M*., et al.* (2012). Fear processing and social networking in the absence of a functional amygdala. Biological psychiatry 72, 70-77.

Bender, S., Weisbrod, M., and Resch, F. (2007). Which perspectives can endophenotypes and biological markers offer in the early recognition of schizophrenia? J Neural Transm 114, 1199-1215.

Bullard, S.E., Griss, M., Greene, S., and Gekker, A. (2013). Encyclopedia of Clinical Neuropsychology. Arch Clin Neuropsych 28, 92-92.

Buzsaki, G., and Draguhn, A. (2004). Neuronal oscillations in cortical networks. Science 304, 1926-1929.

Calhoun, V.D., Miller, R., Pearlson, G., and Adali, T. (2014). The Chronnectome: Time-Varying Connectivity Networks as the Next Frontier in fMRI Data Discovery. Neuron 84, 262-274.

Carmona, S., Vilarroya, O., Bielsa, A., Tremols, V., Soliva, J.C., Rovira, M., Tomas, J., Raheb, C., Gispert, J.D., Batlle, S., and Bulbena, A. (2005). Global and regional gray matter reductions in ADHD: A voxel-based morphometric study. Neurosci Lett 389, 88-93.

Castellanos, F.X., Margulies, D.S., Kelly, C., Uddin, L.Q., Ghaffari, M., Kirsch, A., Shaw, D., Shehzad, Z., Di Martino, A., Biswal, B*., et al.* (2008). Cingulate-precuneus interactions: A new locus of dysfunction in adult attention-deficit/hyperactivity disorder. Biol Psychiat 63, 332-337.

Chang, C., and Glover, G.H. (2010). Time-frequency dynamics of resting-state brain connectivity measured with fMRI. Neuroimage 50, 81-98.

Cherkassky, V.L., Kana, R.K., Keller, T.A., and Just, M.A. (2006). Functional connectivity in a baseline resting-state network in autism. Neuroreport 17, 1687-1690.

Christoff, K., Gordon, A.M., Smallwood, J., Smith, R., and Schooler, J.W. (2009). Experience sampling during fMRI reveals default network and executive system contributions to mind wandering. P Natl Acad Sci USA 106, 8719-8724.

Crespi, B., and Badcock, C. (2008). Psychosis and autism as diametrical disorders of the social brain. Behav Brain Sci 31, 241-+.

Cui, Z.X., Zhong, S.Y., Xu, P.F., He, Y., and Gong, G.L. (2013). PANDA: a pipeline toolbox for analyzing brain diffusion images. Front Hum Neurosci 7.

Damaraju, E., Allen, E.A., Belger, A., Ford, J.M., McEwen, S., Mathalon, D.H., Mueller, B.A., Pearlson, G.D., Potkin, S.G., Preda, A*., et al.* (2014). Dynamic functional connectivity analysis reveals transient states of dysconnectivity in schizophrenia. Neuroimage-Clin 5, 298-308.

de Munck, J.C., Goncalves, S.I., Huijboom, L., Kuijer, J.P.A., Pouwels, P.J.W., Heethaar, R.M., and da Silva, F.H.L. (2007). The hemodynamic response of the alpha rhythm: An EEG/fMRI study. Neuroimage 35, 1142-1151.

Deco, G., Jirsa, V., McIntosh, A.R., Sporns, O., and Kotter, R. (2009). Key role of coupling, delay, and noise in resting brain fluctuations. P Natl Acad Sci USA 106, 10302-10307.

Deco, G., Jirsa, V.K., and McIntosh, A.R. (2011). Emerging concepts for the dynamical organization of resting-state activity in the brain. Nat Rev Neurosci 12, 43-56.

Doucet, G., Naveau, M., Petit, L., Zago, L., Crivello, F., Jobard, G., Delcroix, N., Mellet, E., Tzourio-Mazoyer, N., Mazoyer, B., and Joliot, M. (2012). Patterns of hemodynamic low-frequency oscillations in the brain are modulated by the nature of free thought during rest. Neuroimage 59, 3194-3200.

Faisal, A.A., Selen, L.P.J., and Wolpert, D.M. (2008). Noise in the nervous system. Nat Rev Neurosci 9, 292-303.

Freedman, R., Adler, L.E., Gerhardt, G.A., Waldo, M., Baker, N., Rose, G.M., Drebing, C., Nagamoto, H., Bickford-Wimer, P., and Franks, R. (1987). Neurobiological studies of sensory gating in schizophrenia. Schizophrenia bulletin 13, 669-678.

Frost, M.A., and Goebel, R. (2012). Measuring structural-functional correspondence: Spatial variability

of specialised brain regions after macro-anatomical alignment. Neuroimage 59, 1369-1381.

Garrett, D.D., Kovacevic, N., McIntosh, A.R., and Grady, C.L. (2010). Blood Oxygen Level-Dependent Signal Variability Is More than Just Noise. J Neurosci 30, 4914-4921.

Garrett, D.D., Kovacevic, N., McIntosh, A.R., and Grady, C.L. (2011). The Importance of Being Variable. J Neurosci 31, 4496-4503.

Garrett, D.D., Samanez-Larkin, G.R., MacDonald, S.W.S., Lindenberger, U., McIntosh, A.R., and Grady, C.L. (2013). Moment-to-moment brain signal variability: A next frontier in human brain mapping? Neurosci Biobehav R 37, 610-624.

Garrity, A.G., Pearlson, G.D., McKiernan, K., Lloyd, D., Kiehl, K.A., and Calhoun, V.D. (2007). Aberrant "default mode" functional connectivity in schizophrenia. Am J Psychiat 164, 450-457.

Ghosh, A., Rho, Y., McIntosh, A.R., Kotter, R., and Jirsa, V.K. (2008). Noise during Rest Enables the Exploration of the Brain's Dynamic Repertoire. Plos Comput Biol 4.

Gilbert, S.J., Dumontheil, I., Simons, J.S., Frith, C.D., and Burgess, P.W. (2007). Comment on "Wandering minds: The default network and stimulus-independent thought". Science 317, 43-+.

Glahn, D.C., Laird, A.R., Ellison-Wright, I., Thelen, S.M., Robinson, J.L., Lancaster, J.L., Bullmore, E., and Fox, P.T. (2008). Meta-analysis of gray matter anomalies in schizophrenia: application of anatomic likelihood estimation and network analysis. Biological psychiatry 64, 774-781.

Greicius, M.D., Krasnow, B., Reiss, A.L., and Menon, V. (2003). Functional connectivity in the resting brain: A network analysis of the default mode hypothesis. P Natl Acad Sci USA 100, 253-258.

Guo, S., Kendrick, K.M., Yu, R., Wang, H.L.S., and Feng, J. (2014). Key functional circuitry altered in schizophrenia involves parietal regions associated with sense of self. Human brain mapping 35, 123-139.

Hutchison, R.M., Womelsdorf, T., Gati, J.S., Everling, S., and Menon, R.S. (2013). Resting-state networks show dynamic functional connectivity in awake humans and anesthetized macaques. Hum Brain Mapp 34, 2154-2177.

Jones, D.T., Vemuri, P., Murphy, M.C., Gunter, J.L., Senjem, M.L., Machulda, M.M., Przybelski, S.A., Gregg, B.E., Kantarci, K., Knopman, D.S*., et al.* (2012). Non-Stationarity in the "Resting Brain's" Modular Architecture. Plos One 7.

Kang, J., Wang, L., Yan, C.G., Wang, J.H., Liang, X., and He, Y. (2011). Characterizing dynamic functional connectivity in the resting brain using variable parameter regression and Kalman filtering approaches. Neuroimage 56, 1222-1234.

Kennedy, D.P., and Courchesne, E. (2008). The intrinsic functional organization of the brain is altered in autism. Neuroimage 39, 1877-1885.

Kennedy, D.P., Redcay, E., and Courchesne, E. (2006). Failing to deactivate: Resting functional abnormalities in autism. P Natl Acad Sci USA 103, 8275-8280.

Kopell, N.J., Gritton, H.J., Whittington, M.A., and Kramer, M.A. (2014). Beyond the Connectome: The Dynome. Neuron 83, 1319-1328.

Kucyi, A., and Davis, K.D. (2014). Dynamic functional connectivity of the default mode network tracks daydreaming. Neuroimage 100, 471-480.

Laufs, H., Holt, J.L., Elfont, R., Krams, M., Paul, J.S., Krakow, K., and Kleinschmidt, A. (2006). Where the BOLD signal goes when alpha EEG leaves. Neuroimage 31, 1408-1418.

Lippe, S., Kovacevic, N., and McIntosh, A.R. (2009). Differential maturation of brain signal complexity in the human auditory and visual system. Front Hum Neurosci 3.

Liptak, T. (1958). On the combination of independent tests. Magyar Tud Akad Mat Kutato Int Kozl 3, 171-197.

Lukas, S.E., Mendelson, J.H., Benedikt, R.A., and Jones, B. (1986). EEG alpha activity increases during transient episodes of ethanol-induced euphoria. Pharmacol Biochem Behav 25, 889-895.

Ma, S., Calhoun, V.D., Phlypo, R., and Adali, T. (2014). Dynamic changes of spatial functional network connectivity in individuals and schizophrenia patients using independent vector analysis. Neuroimage 90, 196-206.

Majeed, W., Magnuson, M., Hasenkamp, W., Schwarb, H., Schumacher, E.H., Barsalou, L., and Keilholz, S.D. (2011). Spatiotemporal dynamics of low frequency BOLD fluctuations in rats and humans. Neuroimage 54, 1140-1150.

Makris, N., Biederman, J., Valera, E.M., Bush, G., Kaiser, J., Kennedy, D.N., Caviness, V.S., Faraone, S.V., and Seidman, L.J. (2007). Cortical thinning of the attention and executive function networks in adults with Attention-Deficit/Hyperactivity disorder. Cereb Cortex 17, 1364-1375.

Mantini, D., Perrucci, M.G., Cugini, S., Ferretti, A., Romani, G.L., and Del Gratta, C. (2007). Complete artifact removal for EEG recorded during continuous fMRI using independent component analysis. Neuroimage 34, 598-607.

Mason, M.F., Norton, M.I., Van Horn, J.D., Wegner, D.M., Grafton, S.T., and Macrae, C.N. (2007). Wandering minds: The default network and stimulus-independent thought. Science 315, 393-395.

McIntosh, A.R., Kovacevic, N., and Itier, R.J. (2008). Increased Brain Signal Variability Accompanies Lower Behavioral Variability in Development. Plos Comput Biol 4.

Mesulam, M.M. (1998). From sensation to cognition. Brain 121, 1013-1052.

Misic, B., Mills, T., Taylor, M.J., and McIntosh, A.R. (2010). Brain Noise Is Task Dependent and Region Specific. J Neurophysiol 104, 2667-2676.

Mueller, S., Wang, D.H., Fox, M.D., Yeo, B.T.T., Sepulcre, J., Sabuncu, M.R., Shafee, R., Lu, J., and Liu, H.S. (2013). Individual Variability in Functional Connectivity Architecture of the Human Brain. Neuron 77, 586-595.

Niazy, R.K., Beckmann, C.F., Iannetti, G.D., Brady, J.M., and Smith, S.M. (2005). Removal of FMRI environment artifacts from EEG data using optimal basis sets. Neuroimage 28, 720-737.

Paus, T., Zatorre, R.J., Hofle, N., Caramanos, Z., Gotman, J., Petrides, M., and Evans, A.C. (1997). Time-related changes in neural systems underlying attention and arousal during the performance of an auditory vigilance task. J Cognitive Neurosci 9, 392-408.

Pearlson, G.D., Petty, R.G., Ross, C.A., and Tien, A.Y. (1996). Schizophrenia: A disease of heteromodal association cortex? Neuropsychopharmacol 14, 1-17.

Power, J.D., Cohen, A.L., Nelson, S.M., Wig, G.S., Barnes, K.A., Church, J.A., Vogel, A.C., Laumann, T.O., Miezin, F.M., Schlaggar, B.L., and Petersen, S.E. (2011). Functional Network Organization of the Human Brain. Neuron 72, 665-678.

Power, J.D., Mitra, A., Laumann, T.O., Snyder, A.Z., Schlaggar, B.L., and Petersen, S.E. (2014). Methods to detect, characterize, and remove motion artifact in resting state fMRI. Neuroimage 84, 320-341.

Protzner, A.B., Valiante, T.A., Kovacevic, N., Mccormick, C., and Mcandrews, M.P. (2010). Hippocampal signal complexity in mesial temporal lobe epilepsy: a noisy brain is a healthy brain. Arch Ital Biol 148, 289-297.

Rademacher, J., Burgel, U., Geyer, S., Schormann, T., Schleicher, A., Freund, H.J., and Zilles, K. (2001). Variability and asymmetry in the human precentral motor system - A cytoarchitectonic and myeloarchitectonic brain mapping study. Brain 124, 2232-2258.

Samanez-Larkin, G.R., Kuhnen, C.M., Yoo, D.J., and Knutson, B. (2010). Variability in Nucleus Accumbens Activity Mediates Age-Related Suboptimal Financial Risk Taking. J Neurosci 30, 1426-1434.

Sanz-Martin, A., Guevara, M.Á., Amezcua, C., Santana, G., and Hernández-González, M. (2011). Effects of red wine on the electrical activity and functional coupling between prefrontal–parietal cortices in

young men. Appetite 57, 84-93.

Schumann, G., Loth, E., Banaschewski, T., Barbot, A., Barker, G., Buchel, C., Conrod, P.J., Dalley, J.W., Flor, H., Gallinat, J.*, et al.* (2010). The IMAGEN study: reinforcement-related behaviour in normal brain function and psychopathology. Molecular Psychiatry 15, 1128-1139.

Shirer, W.R., Ryali, S., Rykhlevskaia, E., Menon, V., and Greicius, M.D. (2012). Decoding Subject-Driven Cognitive States with Whole-Brain Connectivity Patterns. Cereb Cortex 22, 158-165.

Sonuga-Barke, E.J.S., and Castellanos, F.X. (2007). Spontaneous attentional fluctuations in impaired states and pathological conditions: A neurobiological hypothesis. Neurosci Biobehav R 31, 977-986.

Sotres-Bayon, F., Sierra-Mercado, D., Pardilla-Delgado, E., and Quirk, G.J. (2012). Gating of fear in prelimbic cortex by hippocampal and amygdala inputs. Neuron 76, 804-812.

Sugiura, M., Friston, K.J., Willmes, K., Shah, N.J., Zilles, K., and Fink, G.R. (2007). Analysis of intersubject variability in activation: An application to the incidental episodic retrieval during recognition test. Hum Brain Mapp 28, 49-58.

Tagliazucchi, E., and Laufs, H. (2014). Decoding Wakefulness Levels from Typical fMRI Resting-State Data Reveals Reliable Drifts between Wakefulness and Sleep. Neuron 82, 695-708.

Tzourio-Mazoyer, N., Landeau, B., Papathanassiou, D., Crivello, F., Etard, O., Delcroix, N., Mazoyer, B., and Joliot, M. (2002). Automated anatomical labeling of activations in SPM using a macroscopic anatomical parcellation of the MNI MRI single-subject brain. Neuroimage 15, 273-289.

Van Dijk, K.R.A., Sabuncu, M.R., and Buckner, R.L. (2012). The influence of head motion on intrinsic functional connectivity MRI. Neuroimage 59, 431-438.

Weissman, D.H., Roberts, K.C., Visscher, K.M., and Woldorff, M.G. (2006). The neural bases of momentary lapses in attention. Nature neuroscience 9, 971-978.

Whitfield-Gabrieli, S., and Ford, J.M. (2012). Default mode network activity and connectivity in psychopathology. Annual review of clinical psychology 8, 49-76.

Whitfield-Gabrieli, S., Thermenos, H.W., Milanovic, S., Tsuang, M.T., Faraone, S.V., McCarley, R.W., Shenton, M.E., Green, A.I., Nieto-Castanon, A., LaViolette, P.*, et al.* (2009). Hyperactivity and hyperconnectivity of the default network in schizophrenia and in first-degree relatives of persons with schizophrenia. Proc Natl Acad Sci U S A 106, 1279-1284.

Yu, R.J., Chien, Y.L., Wang, H.L.S., Liu, C.M., Liu, C.C., Hwang, T.J., Hsieh, M.H., Hwu, H.G., and Tseng, W.Y.I. (2014). Frequency-Specific Alternations in the Amplitude of Low-Frequency Fluctuations in

Schizophrenia. Hum Brain Mapp 35, 627-637.

Zalesky, A., Fornito, A., Cocchi, L., Gollo, L.L., and Breakspear, M. (2014). Time-resolved resting-state brain networks. P Natl Acad Sci USA 111, 10341-10346.

Zeng, L.L., Wang, D.H., Fox, M.D., Sabuncu, M., Hu, D.W., Ge, M., Buckner, R.L., and Liu, H.S. (2014). Neurobiological basis of head motion in brain imaging. P Natl Acad Sci USA 111, 6058-6062.